Fast calculation of electromagnetic scattering in anisotropic multilayers and its inverse problem

Giacomo Rodeghiero, Ping-Ping Ding, Yu Zhong, Marc Lambert, Dominique Lesselier

Fast Calculation of Electromagnetic Scattering in Anisotropic Multilayers and its Inverse Problem

P.-P. Ding[1] G. Rodeghiero[1] Y. Zhong[2,3] M. Lambert[1] **D. Lesselier**[1]

Cooperative works among
[1] Laboratoire des Signaux et Systèmes UMR 8506 (CNRS-SUPELEC-Univ. Paris-Sud)
[2] presently in Institute of High Performance Computing, Singapore
[3] formerly in National University of Singapore (NUS) [1]

ENDE Xi'an June 2014

1. **Special thanks to X. Chen from NUS**

Electromagnetic modeling of fiber-based composite structures

$\Longrightarrow$

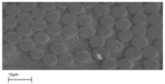

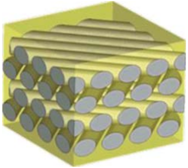

Motivation

- Accurate computational models of complex anisotropic multilayered composite structures
- Robust, fast, end-user's friendly imaging procedures

Forward modeling

$$\bar{\bar{\epsilon}}_r = \text{diag}\left[\bar{\bar{\epsilon}}_{r11} \quad \bar{\bar{\epsilon}}_{r22} \quad \bar{\bar{\epsilon}}_{r22}\right]$$

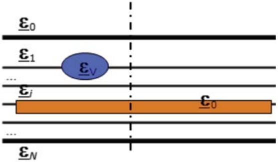

FIGURE: Damaged structure with uniaxial dielectric (glass-based) or conductive (graphite-based) multilayers

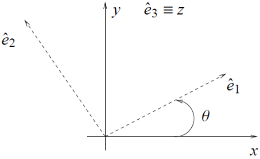

FIGURE: The transformation between the local and global coordinates by rotation matrix

EM response of anisotropic multilayers to distributed sources

The state equation

$$\frac{d}{dz}\bar{\varphi}(z)=\bar{\bar{A}}_n \cdot \bar{\varphi}(z) + \bar{f}(z)$$

based on the 4-component vector :

$$\bar{\varphi}(k_x,k_y,z) = \begin{bmatrix} k_x\tilde{H}_x(k_x,k_y,z)+k_y\tilde{H}_y(k_x,k_y,z) \\ k_y\tilde{H}_x(k_x,k_y,z)-k_x\tilde{H}_y(k_x,k_y,z) \\ k_x\tilde{E}_x(k_x,k_y,z)+k_y\tilde{E}_y(k_x,k_y,z) \\ k_y\tilde{E}_x(k_x,k_y,z)-k_x\tilde{E}_y(k_x,k_y,z) \end{bmatrix}$$

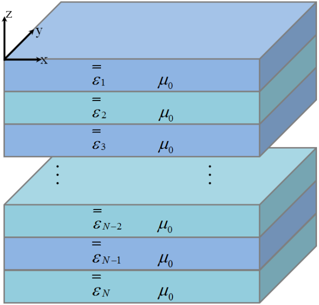

The solution of the state equation

$$\bar{\varphi}(d_{n+1}) = e^{\bar{\bar{A}}_n(\delta_n)} \cdot \bar{\varphi}(d_n) + \int_{d_n}^{d_{n+1}} e^{\bar{\bar{A}}_n(\delta'_n)} \cdot \bar{f}(z')dz'$$

EM response of anisotropic multilayers to distributed sources

The new recurrence equation :

$$\bar{\varphi}\left(d_n\right) = \bar{\bar{\Omega}}_n \cdot \begin{bmatrix} \alpha_n \\ \beta_n \end{bmatrix}$$

New recurrence relations based on the propagator matrix method

- To efficiently calculate the spectral response of the laminate
- Capable of stably dealing with distributed source along z
- More efficient compared to the traditional Green's function method
- To numerically solve the state equation containing the tangential components of the fields

Two methods for calculating the scattered field

1^{st} method

- Induced current integral equation (ICIE)
- windowing technique
- Padua interpolation-integration technique

2^{nd} method

- Lippman-Schwinger integral formula
- Polarization tensor
- Padua interpolation-integration technique

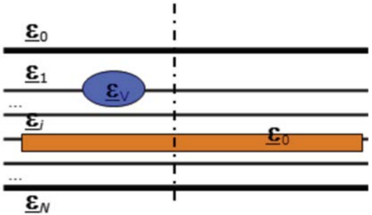

FIGURE: Damaged structure with uniaxial dielectric (glass-based) or conductive (graphite-based) multilayers

Discretization of the integral equation - 1^{st} method

Induced current integral equation (ICIE)

$$\bar{\bar{\chi}}(\mathbf{r}) \cdot \mathbf{E}^{inc}(\mathbf{r}) = \frac{\mathbf{I}(\mathbf{r})}{-i\omega\epsilon_0} - \bar{\bar{\chi}}(\mathbf{r}) \cdot i\omega\mu_0 \int \bar{\bar{G}}(\mathbf{r};\mathbf{r}') \cdot \mathbf{I}(\mathbf{r}')d\mathbf{r}'$$

By MoM

$$\sum_{v=1}^{3} \chi_{u,v;m,n,p} E^{\mathrm{inc}}_{v;m,n,p} = \frac{-1}{i\omega\epsilon_0} \sum_{m',n',p'} I^{(u)}_{m',n',p'} \psi^{(u)}_{m',n',p'}(\boldsymbol{r}_{m,n,p}) - \sum_{v=1}^{3} \chi_{u,v;m,n,p} \sum_{\kappa=1}^{3} \sum_{p'} \sum_{m',n'} \eta_{v\kappa;p;p';(m-m'),(n-n')} I^{(\kappa)}_{m',n',p'}$$

By fast Fourier transform (FFT)

$$\bar{\bar{\xi}}_{v\kappa;p;p'} = \sum_{m',n'} \eta_{v\kappa;p;p';(m-m'),(n-n')} I^{(\kappa)}_{m',n',p'} = \mathrm{IFFT}\left\{\mathrm{FFT}\left\{\bar{\bar{\eta}}_{v\kappa;p;p'}\right\} \otimes \mathrm{FFT}\left\{{}_{(0)}\bar{\bar{I}}^{(\kappa)}_{p'}\right\}\right\}$$

The techniques for calculating the impedance matrix - 1^{st} method

The impedance matrix :

$$\eta_{v\kappa;p;p'}(x,y) = i\omega\mu_0 \int_{\mathcal{D}} G_{v\kappa}\left[(x-x'),(y-y');z_p;z'\right]\psi^{(\kappa)}_{0,0,p'}(\boldsymbol{r}')d\boldsymbol{r}'$$

After detouring the integral path to avoid branch cuts or singularites for the integral involving $\tilde{\eta}_{v\kappa;p;p'}(k_x,k_y)$, the DFT of $\overline{\overline{\eta}}'_{v\kappa;p;p'}$ (the windowed version of $\overline{\overline{\eta}}_{v\kappa;p;p'}$) can be constructed as

$$\hat{\eta}'_{v\kappa;p;p';\alpha,\beta} = \frac{1}{4\pi^2\Delta x\Delta y}\exp\left(i\frac{2\pi\alpha}{M_{\rm t}\Delta x}x_{\rm s} + i\frac{2\pi\beta}{N_{\rm t}\Delta y}y_{\rm s}\right)$$

$$\iint_{-\infty}^{+\infty} d\sigma_x^{\rm R} d\sigma_y^{\rm R}\ \tilde{\eta}_{v\kappa;p;p'}\left[\sigma_x(\sigma_x^{\rm R},\sigma_y^{\rm R}),\sigma_y(\sigma_x^{\rm R},\sigma_y^{\rm R})\right]\left|\frac{\partial(\sigma_x,\sigma_y)}{\partial(\sigma_x^{\rm R},\sigma_y^{\rm R})}\right| \times$$

$$\left\{\sum_{l_1,l_2=-\infty}^{+\infty} e^{i2\pi[l_1(x_{\rm s}/\Delta x)+l_2(y_{\rm s}/\Delta y)]}\tilde{w}\left[\frac{2\pi}{\Delta x}\left(\frac{\alpha}{M_{\rm t}}+l_1\right)-\sigma_x\left(\sigma_x^{\rm R},\sigma_y^{\rm R}\right),\frac{2\pi}{\Delta y}\left(\frac{\beta}{N_{\rm t}}+l_2\right)-\sigma_y\left(\sigma_x^{\rm R},\sigma_y^{\rm R}\right)\right]\right\}$$

2-D Hamming window

$$w(x,y) = \left\{0.54 + 0.46\cos\left[\frac{(x-\Delta x/2)\pi}{a}\right]\right\} \times \left\{0.54 + 0.46\cos\left[\frac{(y-\Delta y/2)\pi}{b}\right]\right\}$$

Padua interpolation-integration technique - calculating fast oscillating integrals

- The goal is to compute the I-FT of fast oscillating spectrum in the $k_x - k_y$ plane

$$G(x,y) = \frac{1}{4\pi^2} \iint_{-\infty}^{\infty} \tilde{G}_0(k_x,k_y) e^{(ik_x x + ik_y y)} \, \mathrm{d}k_x \, \mathrm{d}k_y$$

- Interpolation of the non-oscillating part at the Padua points with Chebyshev's polynomial interpolant

$$\mathcal{L}_n \, \tilde{G}_0(k_x,k_y) = \sum_{k=0}^{n} \sum_{j=0}^{k} c_{j,\,k-j} \, \hat{T}_j(k_x) \, \hat{T}_{k-j}(k_y) - \frac{1}{2} c_{n,0} \, \hat{T}_n(k_x) \, T_0(k_y)$$

  with weights $c_{j,\,k-j}$ computed using [2]
- Fourier transform of Chebyshev polynomials given by

$$\int_{-1}^{1} \hat{T}_n(k_x) \exp(-ik_x x) \, \mathrm{d}k_x$$

  are managed using [3]

2. M. Caliari, S. De Marchi *et al.*, *Numer Algorithms*, **56**, 45-60, 2011
3. V. Dominguez, I. G. Graham *et al.*, *IMA J Numer Anal*, **31**, 1253-1280, 2011

Padua interpolation-integration technique - calculating fast oscillating integrals

Alternative representation as self intersections and boundary contacts of the generating curve $\gamma(t) = (-\cos((n+1)t), -\cos(nt), \; t \in [0, \pi])$

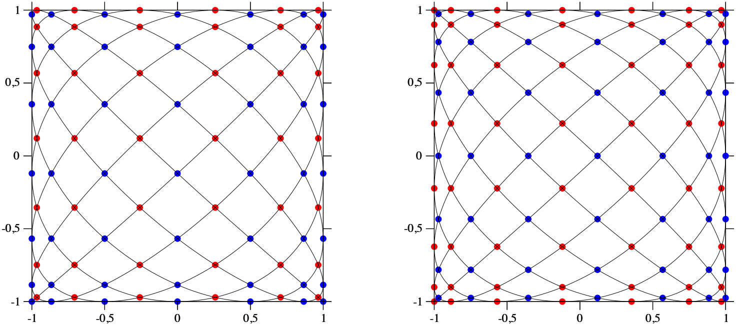

FIGURE: The Padua points with their generating curve for $n = 12$ (left, 91 points) and $n = 13$ (right, 105 points), also as union of two Chebyshev-Lobatto sub-grids (red and blue bullets). Image taken from [5]

M. Caliari, S. De Marchi *et al.*, 5th European Congress of Mathematics - Amsterdam, July, 2008

Fast calculation of EM scattering problems - 2^{nd} method

The Lippman-Schwinger integral formulation

$$\mathbf{E}^{sca}(\mathbf{r}) = i\omega\mu_0 \int \bar{\bar{G}}^{ee}(\mathbf{r},\mathbf{r}') \cdot \bar{\bar{\chi}}(\mathbf{r}') \cdot \mathbf{E}^{tot}(\mathbf{r}')\, \mathrm{d}\mathbf{r}'$$

where the contrast function

$$\bar{\bar{\chi}}(\mathbf{r}) = -i\omega\epsilon_0 \cdot \left(\bar{\bar{\epsilon}}_i - \bar{\bar{\epsilon}}_b\right)$$

$\bar{\bar{\epsilon}}_i$ is the permittivity tensor of an inclusion in the composite medium.
$\bar{\bar{\epsilon}}_b$ is the permittivity tensor of the composite medium in the global coordinate system.

The incident field is defined as

$$\begin{aligned}\mathbf{E}^{inc}(\mathbf{r}) &= i\omega\mu_0 \int \bar{\bar{G}}^{ee}(\mathbf{r},\mathbf{r}') \cdot \mathbf{J}_0(\mathbf{r}')\, \mathrm{d}\mathbf{r}' \\ &= i\omega\mu_0 \bar{\bar{G}}^{ee}(\mathbf{r},\mathbf{r}') \cdot \beta I l\end{aligned}$$

Asymptotic formulation with polarization tensor - 2^{nd} method

The Lippman-Schwinger integral formulation

When permittivity tensor of the inclusion $\bar{\bar{\epsilon}}_i = \bar{\bar{I}}\epsilon_i$ and its size is small enough, the scattered field can be derived into the asymptotic formulation.

$$\mathbf{E}^{sca}(\mathbf{r}) = i\omega\mu_0 \bar{\bar{G}}^{ee}(\mathbf{r}, \mathbf{r}_m) \cdot \bar{\bar{\varrho}} \cdot \mathbf{E}^{inc}(\mathbf{r}_m)$$

The polarization tensor

The polarization tensor in the local coordinate for the inclusion with volume V is :

$$\bar{\bar{\varrho}} = -i\omega\epsilon_0 V \cdot \begin{bmatrix} \alpha_l & 0 & 0 \\ 0 & \alpha_t & 0 \\ 0 & 0 & \alpha_t \end{bmatrix}$$

$$\alpha_l = \epsilon_{11} \frac{\epsilon_i - \epsilon_{11}}{\epsilon_{11} + L_l(\epsilon_i - \epsilon_{11})}$$

$$\alpha_t = \epsilon_{22} \frac{\epsilon_i - \epsilon_{22}}{\epsilon_{22} + L_t(\epsilon_i - \epsilon_{22})}$$

- L_l and L_t are dependent on the shape of inclusion.
- For a cubic inclusion, $L_l = c \arctan\left(c / \sqrt{1+2c}\right)$ and $L_t = (1 - L_l)/2$, where $c = \epsilon_{11}/\epsilon_{22}$ [6].

6. W. S. Weiglhofer and A. Lakhtakia, *Int. J. Infrared Millimeter Waves*, **17**, 1365–1376, 1996.

Comparison of the scattered field by MoM and COMSOL - 1^{st} Case

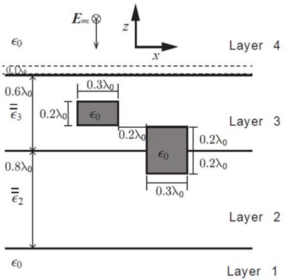

FIGURE: The Configuration of the 1^{st} Case [7]

- freq=6 GHz
- $\bar{\bar{\epsilon}}_2 = \epsilon_0 \,\mathrm{diag}\,[3, 2, 2]$, rotation angle $\theta_2 = 30^\circ$
- $\bar{\bar{\epsilon}}_3 = \epsilon_0 \,\mathrm{diag}\,[4, 2.5, 2.5]$, rotation angle $\theta_3 = 60^\circ$

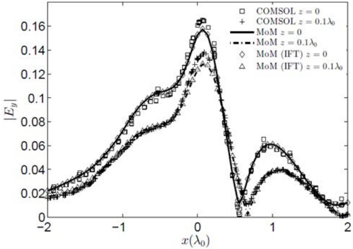

(a) Scattered electric fields along the x-axis.

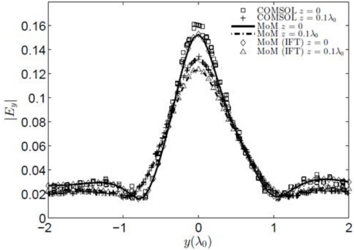

(b) Scattered electric fields along the y-axis.

7. Y. Zhong, P.-P. Ding, M. Lambert, D. Lesselier, and X. Chen, Fast calculation of scattering by 3-D inhomogeneities in uniaxial anisotropic multilayers, *submitted to IEEE Trans. Antennas Propagat.*, 2014.

Comparison of the scattered field by MoM and asymptotic method - 2^{nd} Case

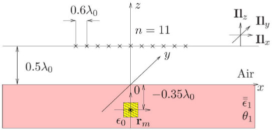

FIGURE: The Configuration of the 2^{nd} Case

- freq=3 GHz
- $\bar{\bar{\epsilon}}_1 =$ ϵ_0 diag $[2 + i0.3, 3 + i0.1, 3 +$
- rotation angle $\theta = 60°$
- 11 electric dipole sources with x/y/z polarization
- a cubic air scatterer with side length $0.1\lambda_0$

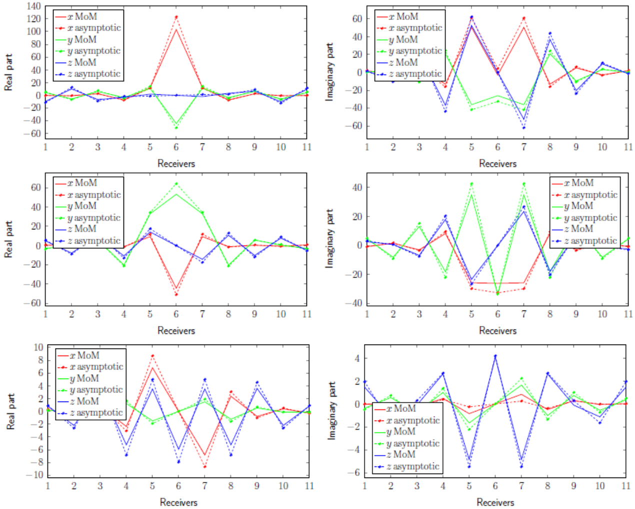

FIGURE: The scattered electric field with sources in x/y/z-polarization

Comparison of the scattered field by MoM and asymptotic method - 3^{rd} Case

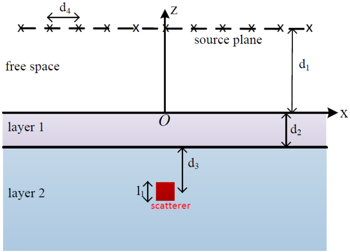

FIGURE: The Configuration of the 3^{rd} Case

- freq = 3 GHz
- $d_1 = 0.5\lambda_0$; $d_2 = 0.2\lambda_0$; $d_3 = 0.35\lambda_0$; $d_4 = 0.2\lambda_0$
- layer 1 : $\bar{\bar{\epsilon}}_1 = \epsilon_0 diag\,[2 + i0.3, 3 + i0.1, 3 + i0.1]$; rotation angle $\theta_1 = 60°$
- layer 2 : $\bar{\bar{\epsilon}}_2 = \epsilon_0 diag\,[4.5 + i0.2, 6 + i0.05, 6 + i0.05]$; rotation angle $\theta_2 = 45°$
- 11 electric dipole sources with x polarization
- a cubic air scatterer with side length $0.1\lambda_0$

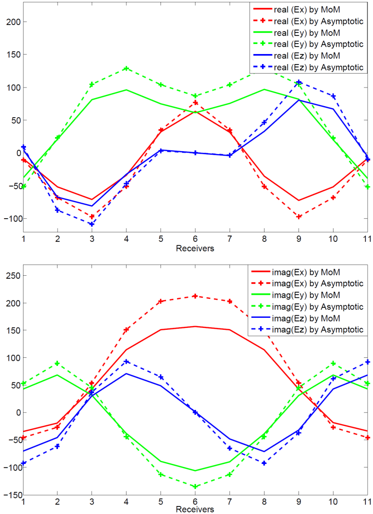

FIGURE: The scattered electric field with the x-polarization source located at $(0, 0, 0.5\lambda_0)$

MUSIC (MUltiple SIgnal Classification) imaging method

Singular value decomposition

$$\mathbf{K} = \mathbf{U}\,\mathbf{S}\,\mathbf{V}^*$$

- Multistatic response matrix **K** maps the currents at the source locations to the scattered fields measured at the detectors.
- Subspace is spanned by the singular vectors corresponding to different singular values.

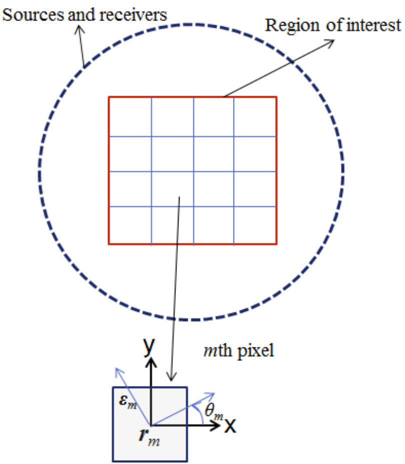

FIGURE: Damaged structure with uniaxial dielectric (glass-based) or conductive (graphite-based) multilayers

MUSIC (MUltiple SIgnal Classification) imaging method

Formulations

Standard MUSIC imaging method [8]

$$\phi(\mathbf{r}) = \frac{1}{\sum_{\sigma_j<\sigma_L} \sum_{v=1}^{3} \left| \bar{u}_j^* \cdot \bar{G}_v(\mathbf{r}) \right|^2}$$

Enhanced MUSIC imaging method [9]

$$\phi(\mathbf{r}) = \frac{1}{1 - \sum_{\sigma_j>\sigma_L} \left| \bar{u}_j^* \cdot \bar{\bar{G}}(\mathbf{r}) \cdot \bar{a}_{\text{test}} \right|^2}$$

with

$$\bar{a}_{\text{test}} = \arg\max_{\bar{a}} \frac{\sum_{\sigma_j>\sigma_L} \left| \bar{u}_j^* \cdot \bar{\bar{G}}(\mathbf{r}) \cdot \bar{a} \right|^2}{\left| \bar{\bar{G}}(\mathbf{r}) \cdot \bar{a} \right|^2}$$

Choice of σ_L

- σ_i being ordered from the largest to the lowest value
- A threshold T arbitrarily chosen

$$\sigma_L = T \times \max_i (\sigma_i) \qquad (1)$$

Exemple for two scatterers $T = 10^3$

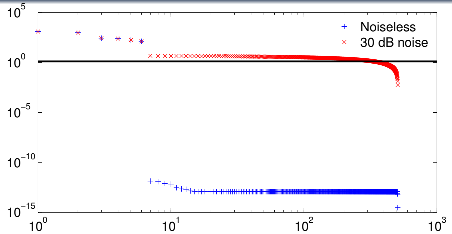

Configuration of interest

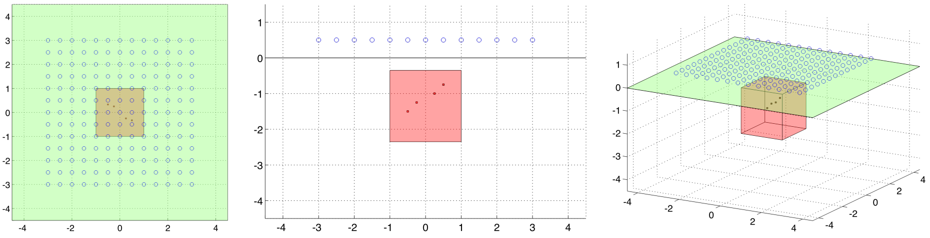

(a) Top view (b) Side view (c) 3D view

FIGURE: Testing configuration

Description of the configuration

Measurement configuration

- location of sources = location of receivers (x/y/z polarization)
- $N_{\text{receivers}} = 13 \times 13$
- z position of receivers : $0.5\lambda_0$
- range of receivers in x-y plane : $[-3\lambda_0, 3\lambda_0]$

Region of interest (ROI)

- $N_{\text{cells}} = 21 \times 21 \times 21$
- range of ROI along z : $[-2.35\lambda_0, -0.35\lambda_0]$
- range of ROI in x-y plane : $[-\lambda_0, \lambda_0]$

The 1^{st} case - one scatterer

plane cut representation

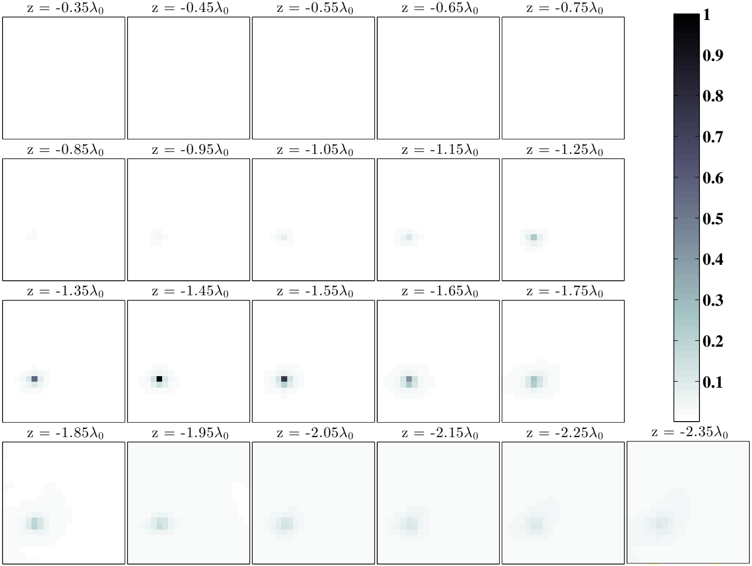

The 1^{st} case - one scatterer

Isosurface = 0.5

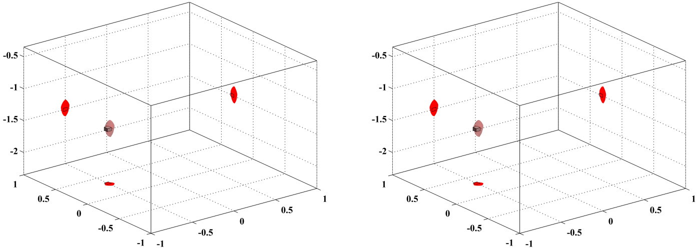

FIGURE: Imaging results by MUSIC for noiseless case (left figure) and 30 dB noisy case (right figure)

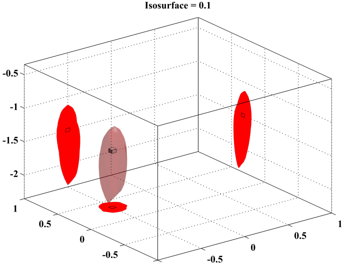

FIGURE: Influence of the choice of the isosurface

The 2^{nd} case - two scatterers

Isosurface = 0.5

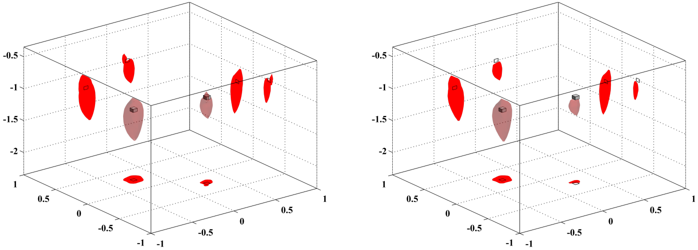

FIGURE: Imaging results by MUSIC for noiseless case (left figure) and 30 dB noisy case (right figure)

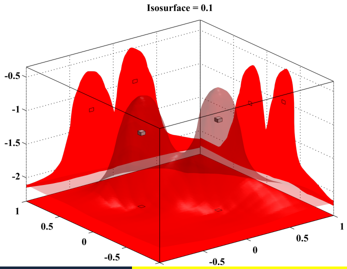

FIGURE: Influence of the choice of the isosurface

The 3^{rd} case - three scatterers

Isosurface = 0.1

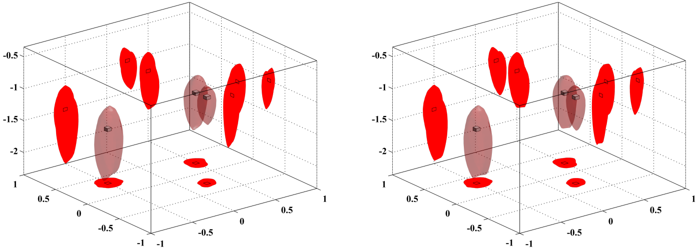

FIGURE: Imaging results by MUSIC for noiseless case (left figure) and 30 dB noisy case (right figure)

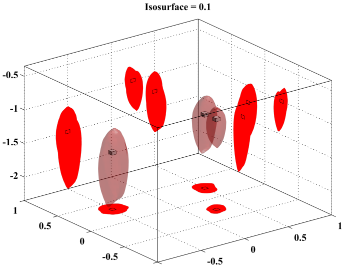

FIGURE: Influence of the choice of the isosurface

The 4^{th} case - four scatterers

Isosurface = 0.1

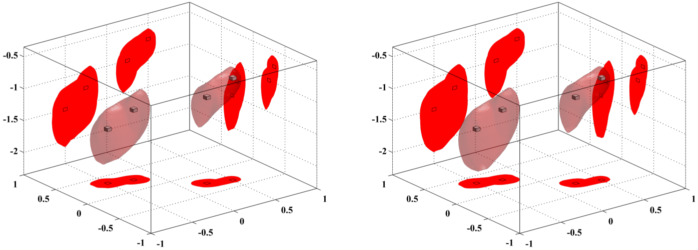

FIGURE: Imaging results by MUSIC for noiseless case (left figure) and 30 dB noisy case (right figure)

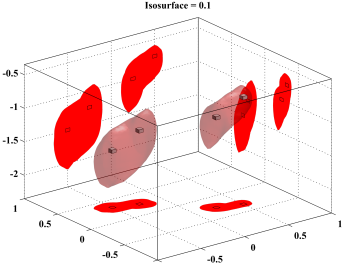

FIGURE: Influence of the choice of the isosurface

Conclusions

Achievements

- Generalized and complete formulation of EM response & Green dyads for undamaged anisotropic multilayers (work at the whole range of frequency for all materials)
- Asymptotic formula-based calculation of EM response for 3-D damaged uniaxial multilayers

Challenges

- To speed up the interpolation and integration for large source-receiver arrays
- To handle delaminations at the interfaces as thin planar defects
- To extend NdT to detecting larger defects by using MUSIC as the first localization tool for non-linearized procedures
- To check the size range of defects possibly detected by the first-order modeling
- To put more endeavor on experiments for practical applications

Thank you & Questions?